Research Paper

PAIN®

# A multi-target approach for pain treatment: dual inhibition of fatty acid amide hydrolase and TRPV1 in a rat model of osteoarthritis

Natalia Malek[a,b], Monika Mrugala[a], Wioletta Makuch[b], Natalia Kolosowska[b], Barbara Przewlocka[b], Marcin Binkowski[c], Martyna Czaja[c], Enrico Morera[d], Vincenzo Di Marzo[e], Katarzyna Starowicz[a,b,*]

**Abstract**

The pharmacological inhibition of anandamide (AEA) hydrolysis by fatty acid amide hydrolase (FAAH) attenuates pain in animal models of osteoarthritis (OA) but has failed in clinical trials. This may have occurred because AEA also activates transient receptor potential vanilloid type 1 (TRPV1), which contributes to pain development. Therefore, we investigated the effectiveness of the dual FAAH–TRPV1 blocker OMDM-198 in an MIA-model of osteoarthritic pain. We first investigated the MIA-induced model of OA by (1) characterizing the pain phenotype and degenerative changes within the joint using X-ray microtomography and (2) evaluating nerve injury and inflammation marker (ATF-3 and IL-6) expression in the lumbar dorsal root ganglia of osteoarthritic rats and differences in gene and protein expression of the cannabinoid $CB_1$ receptors FAAH and TRPV1. Furthermore, we compared OMDM-198 with compounds acting exclusively on FAAH or TRPV1. Osteoarthritis was accompanied by the fragmentation of bone microstructure and destroyed cartilage. An increase of the mRNA levels of ATF3 and IL-6 and an upregulation of AEA receptors and FAAH in the dorsal root ganglia were observed. OMDM-198 showed antihyperalgesic effects in the OA model, which were comparable with those of a selective TRPV1 antagonist, SB-366,791, and a selective FAAH inhibitor, URB-597. The effect of OMDM-198 was attenuated by the $CB_1$ receptor antagonist, AM-251, and by the nonpungent TRPV1 agonist, olvanil, suggesting its action as an "indirect" $CB_1$ agonist and TRPV1 antagonist. These results suggest an innovative strategy for the treatment of OA, which may yield more satisfactory results than those obtained so far with selective FAAH inhibitors in human OA.

**Keywords:** Endocannabinoid, Anandamide, FAAH, TRPV1, $CB_1$, Osteoarthritis, Pain

## 1. Introduction

Osteoarthritis (OA) is a joint disease that primarily affects middle-aged to elderly individuals and is one of the main reasons for undergoing arthroplasty.[34,72] Its key pathological feature is pain caused by the loss of articular cartilage[25] and bone remodeling.[10,28,44] Although numerous drugs have been approved to treat OA symptoms, a meta-analysis indicated that the clinical effects of pharmacological interventions on OA pain are limited to the first weeks of treatment.[8] Therefore, there is a strong need for novel pharmacological approaches in the treatment of OA.

As progress continues in the understanding of pain pathways, several new targets are being identified: the transient receptor potential vanilloid type 1 (TRPV1)[12,31,61] and the cannabinoid receptors of type 1 and 2 ($CB_1$ and $CB_2$) with their endogenous agonists (endocannabinoids).[2,66] TRPV1 antagonists block pain sensitivity,[12,16,31,32] and TRPV1 polymorphisms are associated with an increased risk of symptomatic knee OA,[74] whereas the inhibition of endocannabinoid inactivation by, eg, fatty acid amide hydrolase (FAAH) is effective for chronic and inflammatory pain.[1,41,65,66] Therefore, both might be attractive pharmacological targets for the treatment of OA pain. Despite the claimed therapeutic potential of TRPV1 antagonists, only a few candidates have progressed through clinical trials because of unpredicted secondary effects such as hyperthermia.[24] Regardless of the analgesic properties of selective FAAH inhibitors in rodent pain models,[11,37,38,53] one such compound failed in an OA pain clinical trial,[33,68] most likely because of the redundancy of the endocannabinoid system.[18,57] Indeed, it has been postulated that TRPV1 activation by the endocannabinoid anandamide and/or other FAAH substrates may reduce the analgesic efficacy of FAAH inhibition.[18] Emerging studies highlight how compounds that inhibit both FAAH and TRPV1 may be more efficacious in pain relief than those targeting only one such protein. A prototype molecule, *N*-arachidonoylserotonin (AA-5-HT), has been characterized[7,22] and reported to be more efficacious than a selective FAAH inhibitor in an animal

*Sponsorships or competing interests that may be relevant to content are disclosed at the end of this article.*

*[a] Laboratory of Pain Pathophysiology, Institute of Pharmacology, Polish Academy of Sciences, Krakow, Poland, [b] Department of Pain Pharmacology, Institute of Pharmacology, Polish Academy of Sciences, Krakow, Poland, [c] X-ray Microtomography Laboratory, Department of Biomedical Computer Systems, Institute of Computer Science, Faculty of Computer and Material Science, University of Silesia, Chorzów, Poland, [d] Department of Chemistry and Technology of Pharmacology, Sapienza University of Rome, Rome, Italy, [e] Endocannabinoid Research Group, Institute of Biomolecular Chemistry—C.N.R., Pozzuoli, Italy*

**Corresponding author. Address: Laboratory of Pain Pathophysiology, Department of Pain Pharmacology, Institute of Pharmacology, Polish Academy of Sciences, ul. Smetna 12, 31-343 Krakow, Poland. Tel.: +48 12 6623398; fax: +48 12 6374500. E-mail address: starow@if-pan.krakow.pl (K. Starowicz).*

*Supplemental digital content is available for this article. Direct URL citations appear in the printed text and are provided in the HTML and PDF versions of this article on the journal's Web site (www.painjournalonline.com).*

*PAIN 156 (2015) 890–903*



*http://dx.doi.org/10.1097/j.pain.0000000000000132*

model of inflammatory pain.[14,46] The chemical unstability of AA-5-HT led to the synthesis of potentially more chemically stable piperazinyl carbamates,[51,55] of which OMDM-198 displayed satisfactory dual FAAH and TRPV1 blocking activities and a similar efficacy as AA-5-HT. Recently, Maione et al.[45] reported that OMDM-198 exhibits antinociceptive, antihyperalgesic, and anti-oedemic actions in acute and inflammatory pain. Thus, a multi-target strategy for chronic pain treatment appears to increase the benefit-to-risk ratio of endocannabinoid-based therapeutics.[68]

On the basis of the unsatisfactory outcome of current OA therapies, we tested the analgesic activity of OMDM-198 in an MIA-induced animal model of OA in comparison with compounds acting selectively on either FAAH or TRPV1. We evaluated the model by characterizing pain phenotype and degenerative changes within the joint using X-ray microtomography (XMT). We then assessed the expression of ATF-3, a sensitive marker for peripheral neuron injury, and the proinflammatory cytokine, IL-6, which plays a role in OA pathophysiology. Finally, we studied differences in the expression of proteins of the endocannabinoid system in the lumbar dorsal root ganglia (DRGs) of OA rats using quantitative polymerase chain reaction (qPCR) and immunohistochemistry.

## 2. Materials and methods

### 2.1. Animals

Male Wistar rats (Charles River, Hamburg, Germany) initially weighing between 225 and 250 g were used for all the experiments. The rats were housed in groups of 5 animals per cage under a 12:12-hour light/dark cycle and had free access to food and water. All of the animals were allowed to acclimatize to their holding cages for 3 to 4 days before any behavioral or surgical procedures were conducted. All the experiments were conducted between 9:00 AM and 12:00 AM. The experiments were performed following the guidelines of the IASP[75] and with the approval number 938/2012 of the Local Bioethics Committee of the Institute of Pharmacology (Krakow, Poland). Care was taken to reduce both the number of animals used and the suffering during the experiments.

### 2.2. Drugs and reagents

MIA, URB-597, AM-251, olvanil, and SB-366,791 were obtained from Tocris Bioscience (Bristol, United Kingdom); dimethyl sulfoxide (DMSO), Cremophor and Tween 80 were obtained from Sigma-Aldrich (Poznan, Poland). The OMDM-198 was synthesized, purified, and characterized as described previously.[50] All the reagents were dissolved in a vehicle solution. The vehicle for URB-597 was 2% DMSO, 1% Tween 80, and 1% carboxymethyl cellulose in 0.9% saline. The vehicle for OMDM-198 was 9% DMSO in 0.9% saline. The vehicle for AM-251 and SB-366,791 was 18% DMSO, 1% ethanol, and 1% Tween 80 in 0.9% saline. The vehicle for MIA was 0.9% saline.

### 2.3. Induction of osteoarthritis and assessment of pain-related behaviors

#### 2.3.1. Induction of osteoarthritis

The rats were deeply anesthetized with 2% isoflurane in 100% $O_2$ (1.5 L/min) until the flexor withdrawal reflex was abolished. The skin overlying the right knee joint was shaved and swabbed with 100% ethanol. A 27-gauge needle was introduced into the joint cavity through the patellar ligament, and 50 μL of 0.3 or 3 mg of MIA, which is an irreversible NADPH inhibitor, in 0.9% saline was injected into the joint (intra-articular) to induce OA-like lesions. MIA inhibits chondrocyte glycolysis and produces histological alterations with similarities to clinical histopathology.[20,36]

#### 2.3.2. Dynamic weight bearing

Pain was measured in the MIA-induced model of OA using dynamic weight bearing ([DWB], Bioseb, France) for incapacitance testing in freely moving rats. This system is based on an instrumented floor cage and a combined video acquisition. The rats were placed on a Plexiglas enclosure with a floor composed of sensors (details described in Ref. 63,71). A camera was placed to the side of the enclosure. The rat was allowed to move freely within the apparatus for 5 minutes while the pressure data and live recording were transmitted to a personal computer through a USB interface. Raw pressure and visual data were colligated with the DWB software v1.3. A zone was considered valid when the following parameters were detected: ≥4 g on one sensors with a minimum of 2 adjacent sensors recording ≥1 g. For each time segment in which the weight distribution was stable for more than 0.5 seconds, zones that met the minimal criteria were then validated and assigned as either right or left hind paw or right or left front paw by an observer according to the video and the scaled map of the activated sensors. Other detected zones (tail, testicles, etc.) were also validated but were excluded from analysis. Finally, a mean value for the weight borne by the hind limb and surface area of the hind paw were calculated for the entire testing period based on the length of time of each validated segment. These values were used to calculate the ratio of ipsilateral to contralateral hind paw weight (in grams) and hind paw print area (in square millimeters). The animals were not acclimatized to the enclosure before the initial testing period to maximize exploration behavior.

#### 2.3.3. Pressure application measurement

The pressure application measurement (PAM) device (PAM; Ugo Basile, Italy) has been used for the mechanical stimulation and assessment of joint pain. A quantifiable force was applied for direct stimulation of the joint, and the automatic readout of the response was recorded.[3,42] The animals were held lightly, and the operator placed a thumb with a force transducer mounted unit (circular contact 8 mm, joint surface area of 50.3 $mm^2$) on one side of the animal's knee joint and a forefinger on the other. A gradually increasing squeeze force was applied across the joint at a rate of approximately 300 g/s with a maximum test duration of 15 seconds. Using calibrated instrumentation, the force in grams applied was displayed on a digital screen and was recorded. The test end point was the point at which the animal withdrew its limb or showed any behavioral signs of discomfort or distress, such as freezing of whisker movement or wriggling. Any motion to attempt to withdraw from the device was transferred from the rat limb to the operator's fingers and forearm and was considered an indication of the test end point. On rare occasions, the first sign of distress was shown as the animal vocalizing before limb withdrawal, and on these occasions, this was considered the test end point. The peak gram force (gf) applied immediately before the limb base unit recorded withdrawal, and this value was designated as the limb withdrawal threshold (LWT). Two measurements of both the ipsilateral and contralateral limbs were obtained at 1-minute intervals during which the animals were returned to their respective cages. The mean LWTs were

calculated. Additionally, results were calculated to be presented as Newton per square meter using the conversion factor 0.009814 for Krakow (Poland) geographical location.

The experimenter was blinded to the treatments of both the PAM and DWB measurements. The baseline measurements were obtained immediately before the intra-articular injection (postoperative day 0) and then on respective postoperative days.

### 2.4. Treatment paradigm

In an initial study, pain was measured every hour post-dosing with vehicle, the dual FAAH inhibitor, the TRPV1 blocker, or OMDM-198 with doses of 1 mg, 2.5 mg, and 5 mg/kg injected intraperitoneally (i.p.). In a subsequent study, the $CB_1$ receptor antagonist AM-251 (1 mg/kg, i.p.) and the TRPV1 nonpungent agonist olvanil (1 mg/kg, i.p.) were given 15 minutes before OMDM-198 (1 mg/kg, i.p.), with pain measured every 60 minutes after the OMDM-198 administration. To determine the effects of these compounds alone, AM-251 and olvanil were given separately with joint hypersensitivity measured 30 to 300 minutes post-administration. Changes in joint hypersensitivity were compared with the baseline control (osteoarthritic rats treated with vehicle).

### 2.5. TaqMan quantitative real-time polymerase chain reaction

The animals were killed either 2 or 14 days after the MIA injection. A group of naive animals was used as a reference. The L4–L6 DRG samples were placed in individual tubes with the tissue storage reagent RNAlater (Qiagen Inc), frozen on dry ice and stored at −80°C until RNA isolation. The samples were homogenized in 1 mL of Trizol reagent (Invitrogen, Carlsbad, CA). The RNA isolation was performed according to the manufacturer's protocol. The total RNA quantity was assessed using a Nanodrop spectrophotometer (ND-1000, Nanodrop; Labtech International, United Kingdom). Each sample were equalized to a concentration of 1 μg/μL and reverse transcribed to cDNA using the Omniscript Reverse Transcriptase enzyme (Qiagen Inc) according to the manufacturer's protocol. The reaction was conducted in the presence of the RNase inhibitor rRNAsin (Promega), and an oligo($dT_{16}$) primer (Qiagen Inc) was used to selectively amplify mRNA. The qPCR reactions were performed using Assay-On-Demand TaqMan (Applied Biosystems). The following assays were performed: Rn02758689_s1 ($CB_1$), Rn00583117_m1 (Trpv1), Rn00577086_m1 (Faah), Rn00563784_m1 (ATF3), Rn00561420 (IL-6), and Rn01527840_m1 (Hprt). The reactions were run on a Real-Time PCR CFX96 Touch System (Bio-Rad). The expression of the Hpt1 transcript with a stable level between the control and investigated groups was quantified to control for variation in the cDNA amounts. The threshold cycle (CT) value for each gene was normalized with the CT value of Hprt. The abundance of RNA was calculated as $2^{-(\text{normalized threshold cycle})}$.

### 2.6. Animal perfusion and double immunofluorescence labeling

The rats were anesthetized with sodium pentobarbital (60 mg/kg) and perfused through the ascending aorta with 100 mL of 0.9% saline followed by 300 mL of 4% paraformaldehyde in 0.1 M phosphate buffer (PB), pH 7.4. The lumbar L5 DRG was located by tracing the lumbar dorsal roots back to the sciatic nerve. The dissected tissue was postfixed for 2 hours at 4°C, cryoprotected in 30% sucrose in 0.1 M PB for 12 hours at 4°C, and embedded in Tissue Tek (OCT; Miles Inc, Elkhart, IN). Cryosections were cut and thaw-mounted onto Superfrost slides (Menzel, Germany) at a thickness of 10 μm. The sections were processed for immunohistochemistry. The slides were incubated with PBST (0.1 M PB, 0.1% sodium azide, 0.3% Triton X-100, and 0.3 M NaCl) containing 10% normal goat serum for 1 hour at room temperature. A rabbit primary antibody raised to a truncated form of the rat FAAH protein, ΔTM FAAH, comprising amino acids 38 to 579 as described previously,[15,56] was generously provided by Dr Istvan Nagy, Imperial College London, United Kingdom, and was diluted to 1:2000 in PBST. After 3 washes in PB, the FAAH immunofluorescence was revealed by incubation for 2 hours in a mixture of FITC-Avidin D antibodies (cat no. A-2001; Vector Labs), diluted to 1:600 in PBST and further processing according to the manufacturer's protocol (cat no. NEL700001KT; Perkin Elmer). The co-staining of FAAH with TRPV1 (1:100, cat no. GP14100; Neuromics) and NeuN (1:100, cat no. MAB377, Merck Millipore, Poland) was performed subsequent to the TSA procedure for the FAAH antibody. Double immunofluorescence was revealed by incubation for 4 hours in a mixture of goat anti-mouse conjugated with Alexa 633 and goat anti-guinea pig conjugated with Alexa 555 (Cat. no. A21050 and Cat. no. A-21435, Invitrogen) diluted to 1:100 in NGS.

For the triple immunofluorescence for TRPV1/$CB_1$/NeuN, the sections were incubated for 2 days in a mixture of anti-TRPV1 receptors combined with anti-$CB_1$ (cat no. 209550, Merck Millipore, Poland) and anti-NeuN antibodies (all diluted to 1:100 in NGS) at room temperature. After 3 washes in PB, the triple immunofluorescence was revealed by incubation for 4 hours in a mixture of goat anti-mouse conjugated with Alexa 633, goat anti-rabbit conjugated with Alexa 488 and goat anti-guinea pig conjugated with Alexa 555 (cat. no. A21050, cat. no. A-11008, and cat. no. A-21435, Invitrogen) diluted to 1:100 in NGS.

To demonstrate the specificity of the staining, the omission of either the primary antibody or the secondary antibody was performed (data not shown). Additionally, for double immunofluorescence to ensure that there was no cross reaction between the secondary and primary antibodies, incubation of the section with the first primary antibody and the addition of the second secondary antibody was performed. No immunostaining was detected in any of the controls. The animals that were subjected to immunohistochemistry were not behaviorally tested. We aimed to investigate the status of the TRPV1–$CB_1$ receptor system in response to OA-related pain and not to its pharmacological modulation by the TRPV1 and $CB_1$ receptor ligands.

The sections were examined, and the areas of interest were photo documented on a confocal laser scanning microscope, DMRXA2 TCS SP2 (Leica Microsystems, Germany), with a ×20 dry objective lens (Leica) driven by confocal software (Leica), Ar laser 488 (laser line emitted at 488 nm light), Gre/Ne laser (laser line emitted at 543 nm light), and He/Ne laser (laser line emitted at 633 nm light); the background noise of each confocal image was reduced by averaging 8 scans/line and 8 frames/image. To visualize the image details, plates were generated by adjusting the contrast and brightness of the digital images (ImageJ).

Quantification of the mean percentage value of the number of neurons labeled with TRPV1, $CB_1$ and FAAH was performed by 2 independent observers blinded to the experimental protocols. All the neurons (NeuN+ cells) in the field of view were identified, followed by the single-positive (TRPV1+, CB1+, FAAH+) and then double-positive (TRPV1+/CB1+, TRPV1+/FAAH+) neurons, which were counted for a total of 4 randomly selected sections per group.

Based on the required DRG section micrographs, we performed quantification of the mean percentage value of cells presenting the following immunophenotypes: (1) TRPV1+/CB1+, TRPV1+/CB1−, and TRPV1−/CB1+; and (2) TRPV1+/FAAH+, TRPV1+/FAAH-, and TRPV1−/FAAH+. Two independent observers blinded to the experimental protocols evaluated a total of 4 randomly selected sections per group. Single-positive cells (TRPV1+, CB1+, or FAAH+) and double-positive cells (TRPV1+/CB1+ or TRPV1+/FAAH+) were identified. Only cells with neuronal features were considered (the positivity of NeuN was a necessary but not sufficient condition). The number of single-positive cells that were negative for another marker, ie, (1) TRPV1+/CB1− or TRPV1−/CB1+; and (2) TRPV1+/FAAH or TRPV1−/FAAH+, were extracted from the raw data. A value of 100% indicates that all the cells were analyzed but not all the neurons were identified.

### 2.7. X-ray microcomputer tomography

The ex vivo commercial XMT system was used (vltomelx s, GE Sensing & Inspection Technologies, Phoenixlx-ray, Wunstorf, Germany). The scanner in configuration installed in the X-ray Microtomography Lab (University of Silesia, Chorzów, Poland) has 2 X-ray tubes (transmission hp 180 kV and direct 240 kV) and a 16″ flat panel detector (2024 × 2024 pixels, pixel size = 200 μm). The direct tube was used. The XMT scanning parameters were as follows: System GE Phoenix vltomelx s; voltage (kV): 160; current (μA): 45; voxel size (μm × μm × μm): 7986 × 7986 × 7986; number of images: 1600; detector timing (milliseconds): 250; filter Cu: 0.1. Identical canning parameters were applied to all of the samples. The manufacturer's software was used to perform the image acquisition (Datos 2.0lacq) and image reconstruction (Datos 2.0lrec).

Each sample was placed inside the scanner chamber using the same holder, which also held the calibration phantom required for further quantitative measurements of bone mineral density (BMD). Reconstructed cross-sections were stored in the 256 greyscale format (8 bits per voxel) and were processed later by Drishti (open-source Volume Exploration and Presentation Tool by Limaye[43]) to visualize the sample microstructures. The volume of interest (VOI) (100 × 100 × 130 voxels) selected from the entire stack of images was used to calculate histomorphometric parameters based on binarized images (bone volume/total volume: BV/TV, trabecular thickness: Tb.Th, and trabecular number: Tb.N) using CTAn (Skyscan CT-analyzer software, Belgium) and quantitative parameters related to BMD. The data sets that were segmented using ImageJ (Wayne Rasband National Institutes of Health, USA) were processed using a self-developed plug-in to calculate the quantitative parameter hydroxyapatite density (HAD). Hydroxyapatite density was calculated using our own method for BMD measurements with the calibration curve estimated based on the images of the hydroxyapatite calibration phantom scanned concurrently with the specimen. For a detailed description of XMT, please see Refs. 4,5,17,21.

### 2.8. Statistical analysis

The analysis was performed using Prism V.5 (GraphPad Software). Changes in weight distribution and joint pain in the MIA-treated vs saline-treated rats and changes in mRNA in the DRGs of the MIA-treated and saline-treated rats were analyzed using 2-way analyses of variance with a Bonferroni post hoc test. Unless stated otherwise, the data were analyzed using a one-way analysis of variance with Dunnett or Bonferroni multiple comparison test for time course or between-group comparisons, respectively. The data were considered significant only when $P < 0.05$.

## 3. Results

### 3.1. Effects of intra-articular MIA injection on hind limb weight bearing (DWB) and joint hypersensitivity (PAM)

The DWB baseline test measurements were obtained before the MIA injection. There were no significant differences in weight (mean values: −4 ± 2.3 g) or surface ratio (2 ± 3.2 $mm^2$) between the ispilateral and contralateral rear paws (n = 24). The intra-articular injection of 0.3 mg of MIA (n = 8) resulted in a significant but transient decrease in weight bearing on the injected (ipsilateral) hind limb. These decreases were pronounced on days 2 and 7 after the injection (−33 ± 4.5 g and −31 ± 4.6 g, respectively, $P < 0.01$) and returned to near control levels (−3 ± 3.6 g) by 14 days after the injection (**Fig. 1B**). The lower dose of 0.3 mg of MIA provoked a transient decrease in surface distribution between the ipsilateral and contralateral hind limbs on day 2 (−23 ± 3.0 $mm^2$, $P < 0.05$) (**Fig. 1C**). The day 7 and 14 readouts (−10 ± 2.8 $mm^2$ and 2 ± 3.2 $mm^2$) were not different from the controls (saline-injected rats).

Instead, an intra-articular injection of 3 mg of MIA (n = 8) resulted in a significant and persistent decrease in both the weight and surface ratio. A significant reduction in the ipsilateral vs contralateral weight bearing was observed on days 2, 7, and 14 after administration (−66 ± 3.6 g, −64 ± 3.4 g, and −78 ± 5.0 g on respective days, $P < 0.001$). This result was also observed for the surface differences between the MIA-injected (ipsilateral) and contralateral paws (−54 ± 3.4 $mm^2$, −42 ± 3.4 $mm^2$, and −43 ± 3.1 $mm^2$ on days 2, 7, and 14 after MIA injection, respectively, $P < 0.001$).

Joint hypersensitivity was measured by the PAM test, and automatic recordings of LWTs were obtained. Before the induction of joint inflammation (on day 0), the average ipsilateral LWT was 345 ± 9.8 gf (67,313 ± 1912 N/$m^2$) (n = 24), and the average contralateral LWT reading was 351 ± 7.6 gf (68,483 ± 1483 N/$m^2$) (n = 24). After the injection of 0.3 mg of MIA, the average ipsilateral LWT decreased to 290 ± 12.4 gf (56,582 ± 2419 N/$m^2$) (n = 8) by day 2 ($P < 0.01$, **Fig 1A**). The day 7 measurements of joint withdrawal thresholds of the 0.3 mg MIA-treated animals (n = 8) were significantly lower than those of the saline group (n = 8) whose ipsilateral LWT readings were 303 ± 14.5 gf (59,118 ± 2829 N/$m^2$) ($P < 0.05$, **Fig. 1 A**). The day 14 measurements resulted in a slight decrease in LWT for the 0.3 mg MIA-treated rats: 297 ± 7.5 gf (57,947 ± 1463 N/$m^2$) ($P < 0.001$, **Fig. 1A**). There was no hypersensitivity on the contralateral hind paw.

After the injection of 3 mg of MIA, the average ipsilateral LWT decreased to 303 ± 8.8 gf (59,118 ± 1717 N/$m^2$) (n = 8) by day 2 ($P < 0.05$, **Fig 1A**). Along with OA development, the joint withdrawal thresholds of the 3 mg MIA-treated animals (n = 8) were significantly lower than those of the saline group (n = 8), and the ipsilateral LWT readings after the 3 mg of MIA were 245 ± 6.5 gf (47,802 ± 1268 N/$m^2$) and 220 ± 5.0 gf (42,924 ± 976 N/$m^2$) ($P < 0.001$ for both records, **Fig. 1A**) on days 7 and 14, respectively. Again, there was no hypersensitivity on the contralateral hind paw.

In summary, a decrease in LWT was noted for both 0.3 and 3 mg of MIA; however, the latter dose evoked more profound, significant, and long-lasting decreases (on days 7 and 14, respectively). Significant development of joint hypersensitivity and

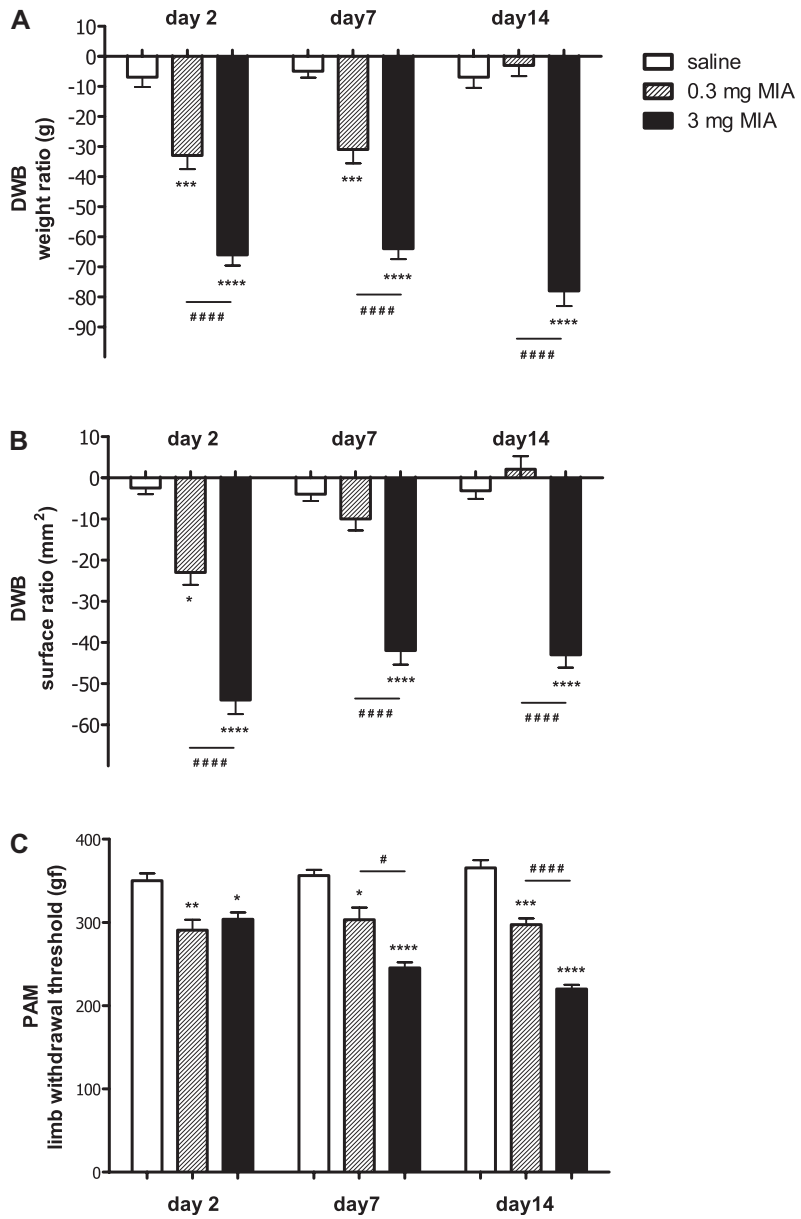


**Figure 1.** Time course and concentration relationship of the effect of intra-articular injection of MIA (0.3 and 3 mg) on hind limb weight bearing (A and B) and joint hypersensitivity (C) in rats. MIA injection resulted in a concentration-dependent weight-bearing impairment recorded as the difference in hind limb dynamic weight bearing in both weight (in grams) and surface (in square millimeters) ratio (ipsilateral–contralateral recordings). Additionally, pressure application measurements of knee joint withdrawal thresholds detected a dose-dependent hypersensitivity. A statistical analysis was performed using a one-way analysis of variance followed by Bonferroni post hoc test. The values with $P < 0.05$ were considered significant. * denotes significance between the MIA- (both doses) and saline-treated groups at the same time point, # denotes significance between the 0.3 and 3 mg MIA-treated groups at the same time point. The values are the means ± SEM.

decreases in weight bearing on the injected hind limb were observed after the 3 mg intra-articular MIA injection; these developments prompted us to use this dose for further experiments and to perform a detailed study of OA pain development.

### *3.2. Behavioral evaluation of MIA-induced knee joint hypersensitivity*

Consistent with previous studies, the time course of weight-bearing asymmetry is biphasic, with the asymmetry slightly correcting at the day 10 time point but returning at day 12.[9,59] To determine knee joint hypersensitivity after a 3 mg MIA injection, measurements were obtained on days 0 to 28. In the rats injected with 3 mg of MIA, the response was biphasic, whereas the activity of the saline-injected control rats was constant from day 0 to day 28 (**Fig. 2**). The ipsilateral LWT after a dose of 3 mg was strongly decreased by day 4 (158 ± 11 gf [30,827 ± 2146 N/m$^2$]) compared with the saline-injected rats (348 ± 9.0 gf [67,898 ± 1756 N/m$^2$]) and returned to control values by days 9 to 10 (304 ± 16.0 gf [59,313 ± 3122 N/m$^2$] and 332 ± 15.0 gf [64,776 ± 2927 N/m$^2$] for the MIA-treated rats vs 342 ± 5.8 gf [66,727 ± 1132 N/m$^2$] and 355 ± 8.0 gf [69,264 ± 1561 N/m$^2$] for the saline-injected rats, respectively). After returning to normal activity levels, the OA rats became progressively hypersensitive to pressure applied to the joint from day 11 to day 28 (the end of the study) (**Fig. 2**).

Because the MIA-induced model of OA allows the evaluation of anti-inflammatory (to treat early symptoms) and analgesic (to treat chronic pain) drugs and because there were no significant

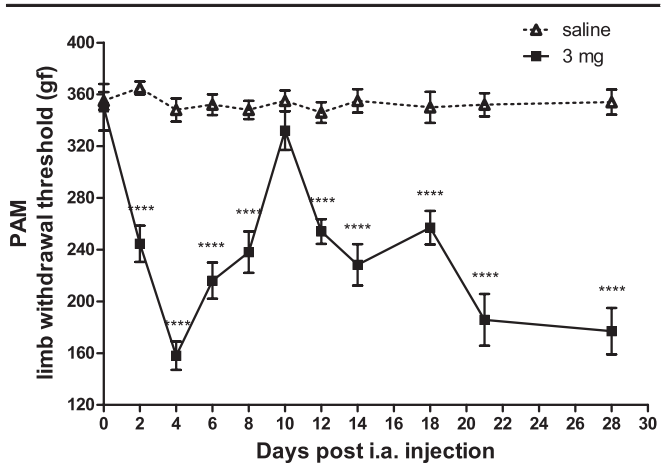


**Figure 2.** The ipsilateral pressure application measurement of limb withdrawal threshold of saline and MIA-treated rats over a 28-day study. MIA injection resulted in a biphasic decrease of the withdrawal threshold of the injected paw with a chronic phase beginning approximately 12 days after the MIA injection. A statistical analysis was performed using a one-way analysis of variance followed by Bonferroni post hoc test. * denotes statistical significance ($P < 0.0001$) between the MIA- and saline-treated groups at the same time point. The values are the means ± SEM.

changes between LWT readouts from day 14 to day 28, day 14 was selected for future studies evaluating the analgesic profile of OMDM-198 to minimize the suffering of the animals. Indeed, consistent with literature data,[9,26] day 14 after MIA injection results in rigorous cartilage destruction and OA-like knee pain. We also confirmed this by XMT (see **Fig. 3** for details).

### 3.3. MIA progression and bone destruction

X-ray microtomographic images of bone microstructure represent quantitative assessments of bone and not direct damage to cartilage structure. The measurement of bone microstructure was performed using the known histomorphometry parameters bone friction (BV/TV), trabecular thickness (Tb.Th), and trabecular number (Th.N), which are based on binarized images. In addition, a method of the absolute value of BMD measurements (HAD) was applied based on calibrated XMT data. The results are presented in **Table 1**.

The bone volume fraction (BV/TV) increased over time because destroyed bone was compacted in the subchondral region of the bone in the joint. Referenced VOI (100 × 100 × 130 voxels) contains bone segmented from the greyscale XMT images (0-255) using threshold and later binary images (0-1) to estimate BV/TV, Tb.Th, and Th.N. An increase in the bone material because of the compacting of destroyed trabecules was observed. An increase in trabecular thickness at day 0 and day 14 and a decrease at day 28 were observed; the trabecular number decreased at day 14 and increased at day 28. The thickness of the trabecules increased, whereas arthritis was not yet visually observed; however, the structure from the entire VOI was affected at day 14. A reverse pattern characterized day 28: the trabecular thickness decreased, whereas the trabecules number increased, suggesting that the microstructure became compacted and the trabecules became thinner.

The HAD parameter was calculated based on calibrated XMT images. The HAD analysis gave the following results: $HAD_{day\ 0}$ = 1.27 mg HA/ccm, $HAD_{day\ 14}$ = 1.17 mg HA/ccm, and $HAD_{day\ 28}$ = 1.30 mg HA/ccm. The BMD estimated using HAD at day 14 was decreasing, most likely as a result of a reduction in bone mineral content as a consequence of early-stage OA development. Along with no changes in BV/TV, the Tb.Th, and Tb.N fluctuations reflected the fact that the XMT bone microstructure image at day 14 had not yet changed. However, BV/TV based on binarized images did not show the decreasing HAD, which would support the loss of subchondral bone.

In conclusion, the results from the HAD measurements follow the increasing values of BV/TV, resulting in a decreasing trend of compacting bone; however, for day 14, the results were less clear. It can be assumed that bone density was decreasing, but the structure had not changed at this time point.

### 3.4. Expression of atf-3 and il-6 on the lumbar L4–L6 dorsal root ganglia of the rats exposed to MIA injection

As a marker of nerve injury and proinflammatory cytokines (catabolic in general) produced by joint tissue and released into the synovial fluid, the mRNA levels of activating transcription factor 3 (*atf-3*) and interleukin 6 (*il-6*) were quantified by real-time qPCR in the lumbar DRG (L4–L6) of normal and OA rats. Significantly increased *atf-3* expression following the MIA treatment was measured in osteoarthritic DRG on days 2, 7, and 14 (**Fig. 4A**, $P < 0.001$) compared with the controls. The OA animals showed a significant increase in *atf-3* expression, which was different from the control animals as early as day 2 (from 1 ± 0.2 to 16.7 ± 0.7 and 11.6 ± 0.8 on the ipsilateral and contralateral sides, respectively). The *atf-3* expression declined slightly until day 14, although it was significantly higher than the baseline expression observed in the control animals (12.4 ± 0.7 vs 9.8 ± 0.9 and 12.2 ± 0.7 vs 8.6 ± 0.8 on the ipsilateral and contralateral sides on days 7 and 14, respectively). Significant differences between the ipsilateral and contralateral sides were also noted for days 2 and 14.

A significant imbalance in *il-6* expression levels was observed in the osteoarthritic rats (**Fig. 4B**) compared with the controls. Baseline *il-6* expression was similar in the control animals and in the contralateral DRG of the OA animals at all time points studied ($P > 0.05$). There was an increase in *il-6* expression in the ipsilateral DRG of the MIA-treated animals. On day 2, an upregulation of *il-6* expression in the ipsilateral lumbar DRG was observed (5.2 ± 0.5, $P < 0.005$), whereas no change was noted on day 7. The unilateral *il-6* upregulation was observed again on day 14 (3.2 ± 0.6, $P < 0.05$).

### 3.5. Changes in cnr1, trpv1 and faah gene expression in the lumbar L4–L6 dorsal root ganglia of the rats exposed to MIA injection

We next determined the changes in *cnr1*, *trpv1*, and *faah* mRNA levels because they represent primary targets for the piperazinyl carbamate and TRPV1/FAAH blockers used here.

The changes in *cnr1* gene expression in the ipsilateral and contralateral sections of the lumbar DRG of the OA rats are shown in **Fig. 5A**. The levels of *cb1* mRNA in the rat L4–L6 DRG were increased by MIA treatment, which is shown by the 3- to 4-fold increase reported in the DRGs (**Fig. 5A**). This increase was observed at all 3 time points tested (upregulation from 1 ± 0.15 to 3.7 ± 0.4, 4.8 ± 0.5, and 4.2 ± 0.4 on the ipsilateral side on days 2, 7, and 14, respectively, $P < 0.001$). Additionally, an analysis of *cnr1* transcript levels revealed that 2 days after the MIA injection, there was an increase observed on the contralateral side as well (4.2 ± 0.4; $P < 0.001$). Significantly higher *cnr1* transcript levels were present on days 7 and 14 in the ipsilateral compared with the contralateral side. An analysis of the transcript levels of *trpv1*

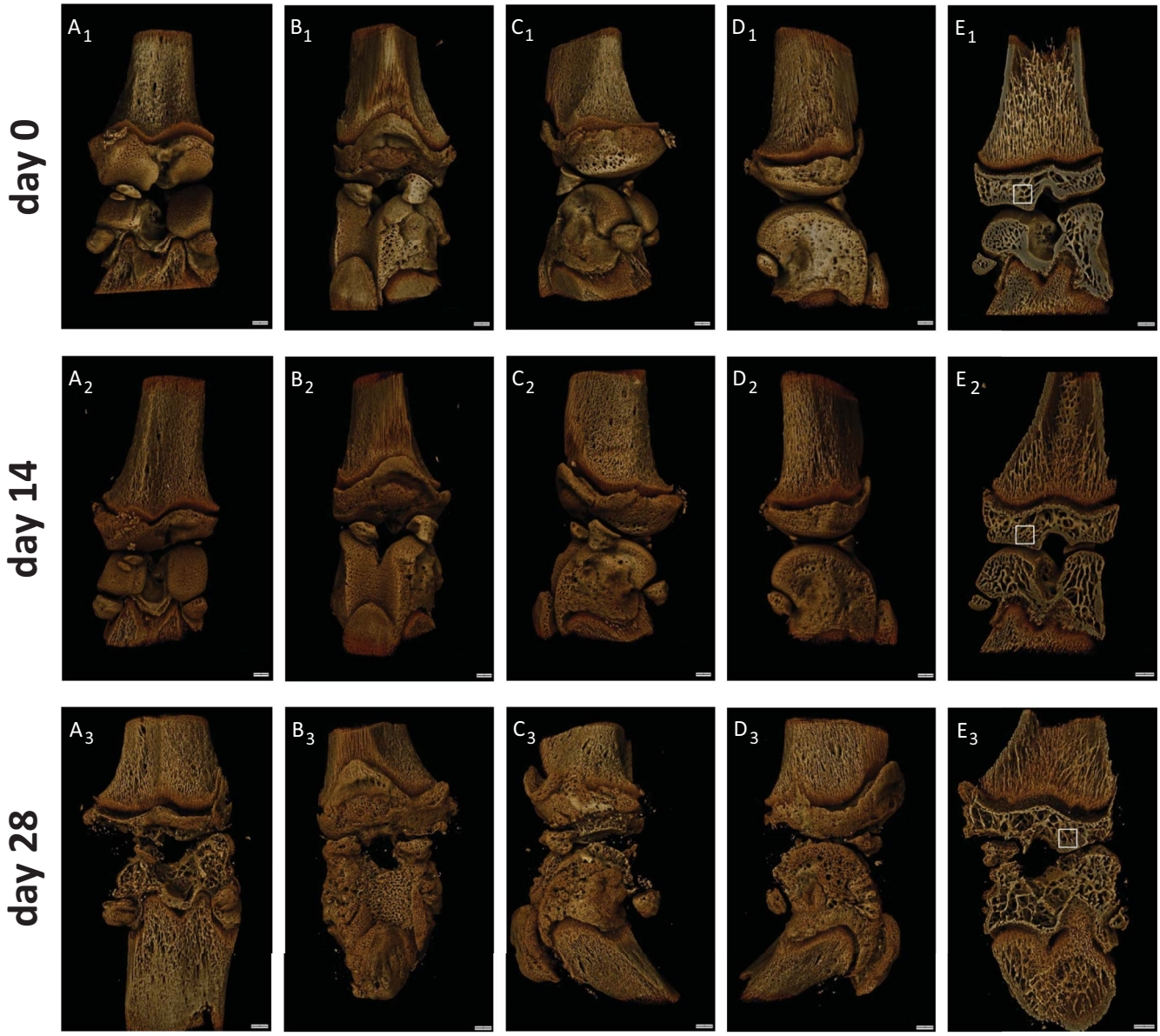


**Figure 3.** X-ray microtomography–based 3-dimensional visualization of the knee joint samples during the development of osteoarthritis pain in the iodoacetate-injected rats (at days 0, 14, and 28). Each sample is presented in an anterior–posterior view ($A_1$-$B_3$), left and right views ($C_1$-$D_3$), and a vertical cross-sectional view ($E_1$-$E_3$) through the joint in the location of the volume of interest (marked by a white rectangle) where the bone fraction (BV/TV) and hydroxyapatite density were calculated.

revealed that its mRNA in the DRG was increased in the ipsilateral side on day 2 after the MIA treatment (1 ± 0.2 vs 1.9 ± 0.1; $P < 0.05$), but the mRNA levels returned to the levels observed in the control animals on days 7 and 14 (**Fig. 5B**). The amount of *faah* mRNA in the DRG was significantly upregulated on day 7 after the MIA injection (1 ± 0.2 vs 2.2 ± 0.2; $P < 0.01$) exclusively in the ipsilateral side (**Fig. 5C**).

**Table 1**

**X-ray microcomputer tomography–based parameters of histomorphometric BMD during the development of OA pain in the iodoacetate-injected rats (at days 0, 14, and 28).**

| | Day 0 | Day 17 | Day 28 |
|---|---|---|---|
| BV/TV, % | 31.36 | 38.43 | 46.66 |
| Tb.Th, mm | 0.031 | 0.047 | 0.037 |
| Tb.N, 1/mm | 9.830 | 8.152 | 12.598 |
| HAD, g HA/cm$^3$ | 1.270 | 1.170 | 1.300 |

BMD, bone mineral density; BV/TV, bone volume/total volume; HAD, hydroxyapatite density; OA, osteoarthritis; Tb.N, trabecular number; Tb.Th, trabecular thickness.

### *3.6. TRPV1, CB1, and FAAH immunoreactivity in dorsal root ganglion neurons*

Approximately 40% of all lumbar (L4/L5) DRGs were TRPV1 positive (40.6% ± 2.4%). Immunohistochemical colocalization of TRPV1 with $CB_1$ or FAAH in rat L5 DRG 14 days after MIA-induced OA was determined by immunofluorescence (**Figs. 6 and 7**). Only cells with neuron characteristics were considered and identified as NeuN-positive cells (**Fig. 6**, $A_1$-$A_2$; **Fig. 7**, $A_1$-$A_2$). In agreement with the results obtained by single staining, we identified many TRPV1-positive (**Fig. 6**, $B_1$-$B_2$; **Fig. 7** $B_1$-$B_2$), $CB_1$-positive (**Fig. 6**, $C_1$-$C_2$), and FAAH-positive (**Fig. 7**, $C_1$-$C_2$) neurons, regardless of the treatment paradigm (MIA-injected

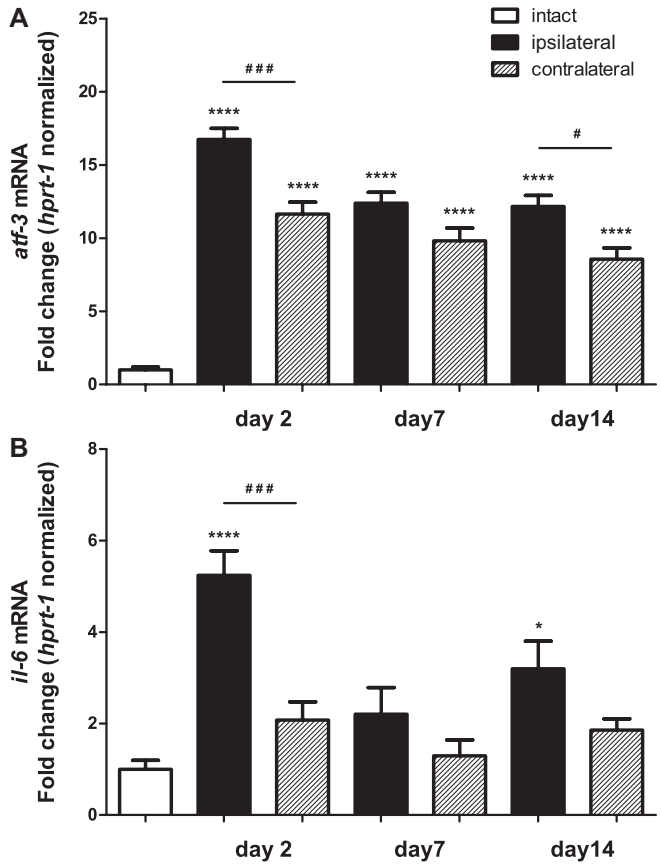


**Figure 4.** Results of the quantitative polymerase chain reaction analysis of *atf-3* (A) and *il-6* (B) gene expression levels in the L4–L6 dorsal root ganglia during the development of osteoarthritis pain in MIA-treated rats. Samples were collected 2, 7, and 14 days after osteoarthritis induction. Data are presented as the means ± SEM and represent the normalized averages derived from 4 to 6 samples for each group. The results are presented as a fold change normalized to the expression of a reference gene, *hprt1*, compared with the intact animals. A Statistical analysis was performed using a one-way analysis of variance followed by Bonferroni post hoc test. Values with $P < 0.05$ were considered significant. * denotes significant differences vs intact, # denotes significant differences vs the contralateral side.

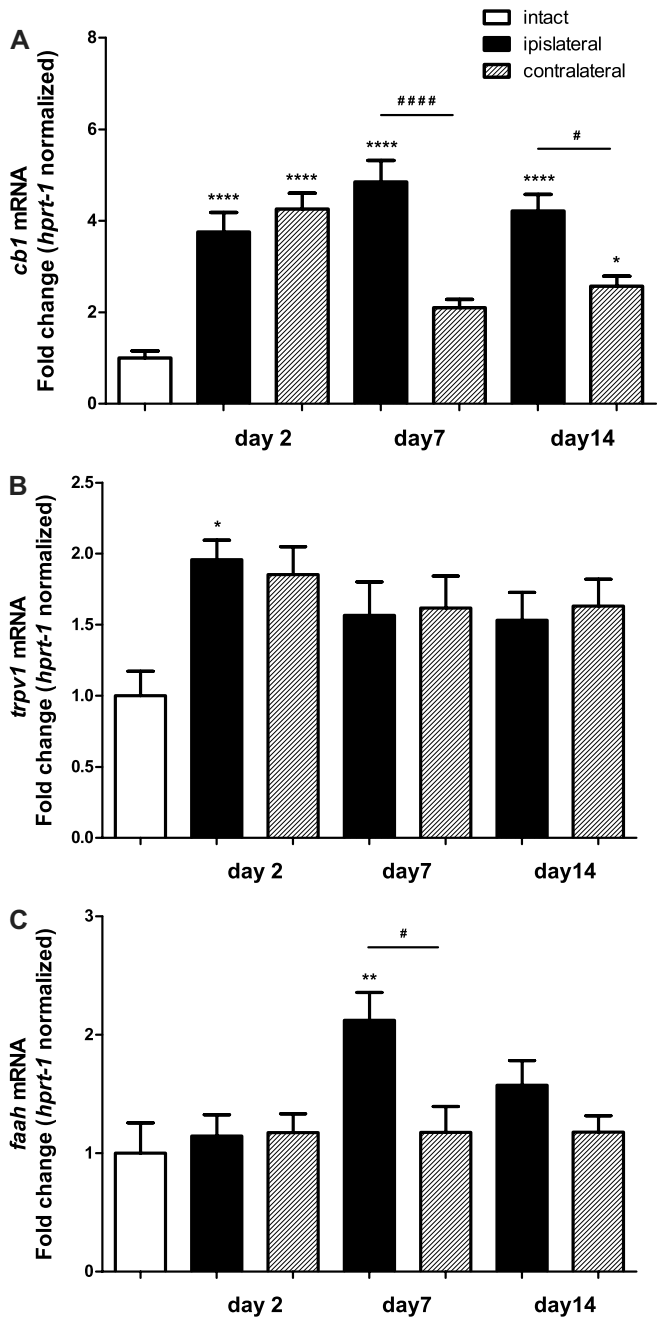


**Figure 5.** Results of the quantitative polymerase chain reaction analyses of *Cnr1* (A), *Trpv1* (B), and *Faah* (C) gene expression levels in the L4–L6 dorsal root ganglia during the development of osteoarthritis pain in MIA-treated rats. Samples were collected 2, 7, and 14 days after osteoarthritis induction. Data are presented as the means ± SEM and represent the normalized averages derived from 4 to 6 samples for each group. The results are presented as a fold change normalized to the expression of a reference gene, *Hprt1*, compared with the intact animals. A statistical analysis was performed using a one-way analysis of variance followed by Bonferroni post hoc test. The values with $P < 0.05$ were considered significant. * denotes significant differences vs intact, # denotes significant differences vs the contralateral side.

knee or not). The staining profiles for the controls (healthy rats) were similar (data not shown). Using double fluorescence, we found that TRPV1 and $CB_1$ receptors that were immunolabeled colocalized largely (**Fig. 6**, $D_1$-$D_2$) and reached approximately 67% (**Fig. 6E**), irrespective of the procedure (data not shown) and lateralization. Furthermore, the number of TRPV1+/$CB_1$− and TRPV1−$CB_1$+ cells did not change in our experimental setting and was approximately 16% (**Fig. 6E**). Similarly, the co-expression of TRPV1 and FAAH was stable and was approximately 67% (**Fig. 7**, $D_1$-$D_2$ and E) with a subsequent constant percentage of TRPV1+/FAAH− and TRPV1−/FAAH+ cells, again reaching approximately 16% (**Fig. 7E**). These data suggest a lack of alteration in $CB_1$, TRPV1, and FAAH protein levels after MIA-induced OA.

### *3.7. The effects of systemic OMDM-198 administration on joint hypersensitivity in MIA-treated rats*

Osteoarthritis was induced in the rats by the intra-articular injection of 3 mg of MIA. The animals were allowed to recover for 14 days, which has consistently been shown to cause cartilage destruction in this species, resulting in OA-like knee pain.[9,26] On day 14, the OA rats were randomly assigned into one of 4 treatment groups: vehicle (n = 8) or OMDM-198–treated groups (1, 2.5, and 5 mg/kg, i.p., each group with n = 8).

The application of vehicle had no significant effect on the pain response as measured in the LWT. A 1 mg/kg (i.p.) dose of OMDM-198 significantly increased the LWT compared with the vehicle-treated group, reflecting an analgesic response up to 120

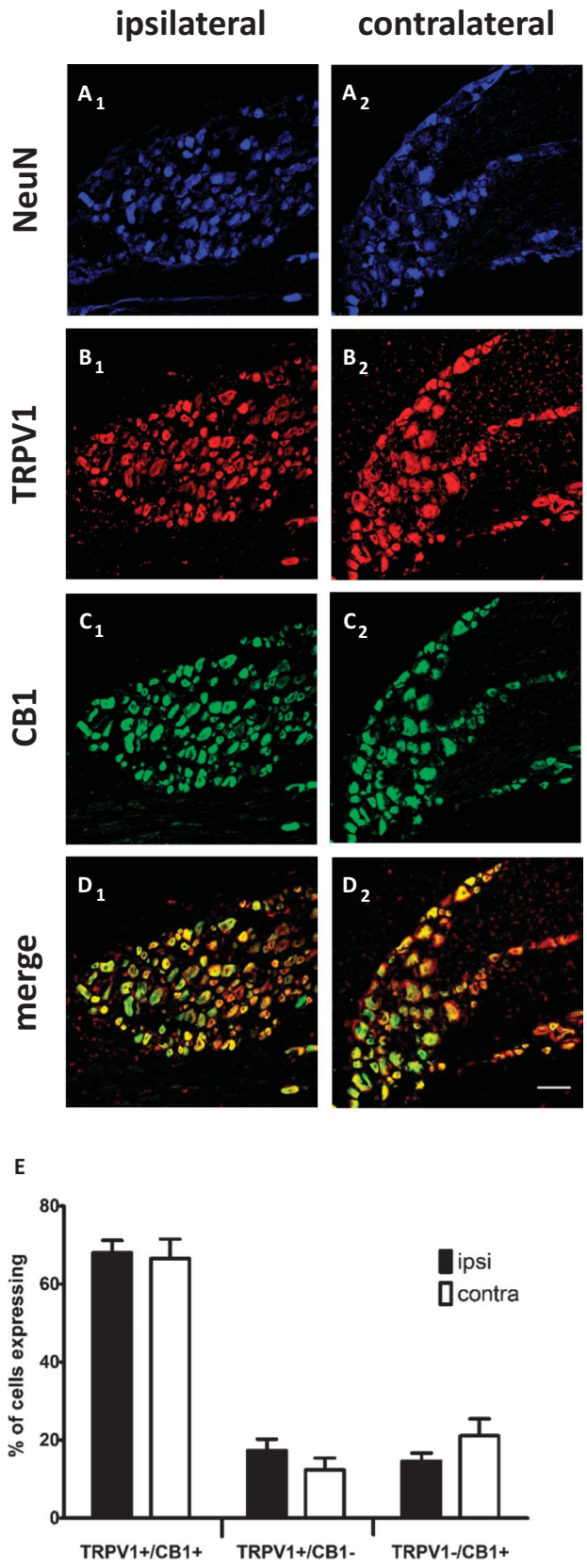


**Figure 6.** Photomicrographic and quantitative representation of TRPV1 and $CB_1$ expression in adult rat L5 dorsal root ganglion (DRG) 14 days after MIA-induced osteoarthritis. L5 DRG sections of osteoarthritis rats (A-D): ipsilateral ($A_1$-$D_1$) and contralateral ($A_2$-$D_2$) to injection. The images represent the distribution of neurons in rat L5 DRG ($A_1$-$A_2$; blue), immunolabeling for TRPV1 ($B_1$-$B_2$; red), immunolabeling for $CB_1$ ($C_1$-$C_2$; green), and merged signals for TRPV1 and $CB_1$ ($D_1$-$D_2$; orange). Different subpopulations of neurons were immunoreactive to TRPV1 and $CB_1$ (E). The data are presented as the % of expressing cells ± SEM. Each column represents the mean of at least 4 areas counted by 2 observers who were blinded to the study. The results were evaluated using a *t* test analysis. No statistical significance ($P < 0.05$) was found. Scale bar = 100 μm.

minutes after administration ($P < 0.05$, $P < 0.001$, and $P < 0.0001$, respectively; **Fig. 8A**). Intriguingly, compared with the vehicle, the effects of OMDM-198 at doses of 2.5 and 5 mg/kg (i.p.) were not significant ($P > 0.05$; **Fig. 8A**).

In a subsequent study, rats (n = 40) were randomly assigned to one of 5 treatment groups: vehicle, OMDM-198, AM-251, olvanil, AM-251 + OMDM-198, and olvanil + OMDM-198. All the drugs were injected intraperitoneally using a 1 mg/kg dose. Each group consisted of n = 8 animals. The systemic administration of the $CB_1$ receptor antagonist AM-251 15 minutes before the administration of OMDM-198 significantly reduced the analgesic capacity of the dual FAAH inhibitor/TRPV1 antagonist ($P < 0.05$ and $P < 0.01$; **Fig. 8B**). AM-251 administered alone had no effect on MIA-evoked pain ($P > 0.05$; **Fig. 8B**). Administration of the TRPV1 receptor nonpungent agonist, olvanil, which exhibited no analgesic action per se, also reduced the 0- to 60-minute analgesic capacity of OMDM-198 ($P < 0.05$; **Fig. 8C**). In the presence of the $CB_2$ receptor antagonist AM630, OMDM-198 still produced significant antinociceptive effects compared with the vehicle (Supplementary Fig. 1, available online as Supplemental Digital Content at http://links.lww.com/PAIN/A49).

### *3.8. Comparison of the OMDM-198 analgesic effect with single-target acting drugs (URB-597 and SB-366,791) on joint hypersensitivity in MIA-treated rats*

A comparison between OMDM-198, URB-597, and SB-366,791 evaluated 60 minutes after administration revealed that all of the drugs were equally potent at inhibiting joint hypersensitivity (**Fig. 9**). However, the molar doses (2.4 μM OMDM-198, 14.8 μM URB-597, and 6.9 μM SB-366,791) required to achieve a comparable analgesic effect were higher for URB-597 (approximately 6.2-fold greater) and SB-366,791 (approximately 2.8-fold greater). No dose of OMDM-198, URB-597, or SB-366,791 affected the LWT of the contralateral paws (data not shown).

## 4. Discussion

The high incidence of OA in the elderly population, along with the increasing age of the general population, indicates that the number of patients suffering from pain associated with this condition will increase and emphasizes the need to validate preclinical models of OA that can be used to assess both the factors contributing to OA pain and the disease-modifying effects of potential therapeutics.

We have characterized an MIA-induced model of OA in relation to the development of pain behavior. An intra-articular injection of 3 mg of MIA induced a sustained decrease in hind limb weight bearing and an increase in joint hypersensitivity. In a human clinical population, OA is not suspected until there has been a significant disease progression, at which time the disease is associated with joint dysfunction and pain. In this study, pain behavior associated with intra-articular MIA injection was biphasic, with the initial phase lasting approximately 8 days and the chronic phase beginning at day 12. As evidenced by XMT, no bone destruction was observed until the chronic phase, further supporting the fact that the majority of damage to articular tissue

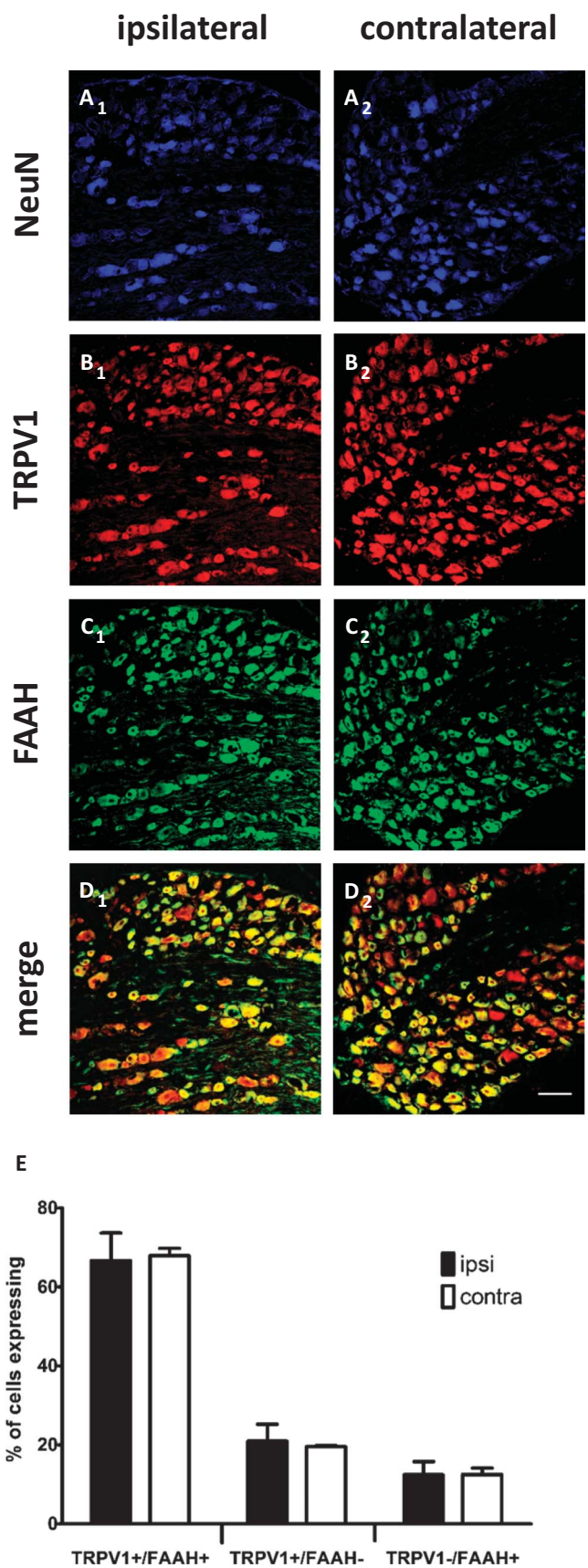


**Figure 7.** Photomicrographic and quantitative representation of TRPV1 and FAAH expression in adult rat L5 dorsal root ganglion (DRG) 14 days after MIA-induced osteoarthritis. L5 DRG sections of osteoarthritis rats (A-D): ipsilateral ($A_1$-$D_1$) and contralateral ($A_2$-$D_2$) to injection. The images represent the distribution of neurons in rat L5 DRG ($A_1$-$A_2$; blue), immunolabeling for TRPV1 ($B_1$-$B_2$; red), immunolabeling for FAAH ($C_1$-$C_2$; green), and merged signals for TRPV1 and FAAH ($D_1$-$D_2$; orange). Different subpopulations of neurons were immunoreactive to TRPV1 and FAAH (E). The data are presented as the % of expressing cells ± SEM. Each column represents the mean of at least 4 areas counted by 2 observers who were blinded to the study. No statistical significance ($P < 0.05$) was found. Scale bar = 100 μm.

in the first 7 days after the MIA injection was to the cartilage, with bone damage not yet present.[27] Although the behavioral changes and histology both worsened over time, the majority of the pain responses were apparent within 7 days of the MIA injection, whereas gross joint damage was not evident by day 14. This mirrors the clinical situation in which patients report pain with no severe joint damage present.[29] Additionally, XMT does not measure cartilage destruction directly; however, it can monitor the quality of subchondral bone, which supports the cartilage. X-ray microtomography demonstrated that intra-articular MIA induced significant alterations in the subchondral bone; additionally, in the same regions of the joint where the changes in the subchondral bone were observed, cartilage loss might also occur.[54]

Cytokines and growth factors are elevated during OA pathogenesis[35]; low levels of many of these factors are necessary for normal homeostasis, but, in OA, their balance may be disturbed. Indeed, IL-6 levels significantly increased as early as 2 days after MIA injection, which may promote OA development and modulate the effects of cytokines such as IL-1β, tumor necrosis factor α, IL-17 or IL-18, which also promote tissue damage. Another study suggested a similarity between OA and neuropathic pain.[35] We observed a strong *atf-3* signal in the L4–L6 DRG in response to MIA between days 2 and 14. Consequently, in this study, increased transcripts of *atf-3* in the L4–L6 DRG might be indicative of neuronal damage[73] and imply that the intra-articular injection of MIA is associated with early neuropathy, as demoinstrated by the fact that IL-6 levels were not significantly different from control levels, the cytokine was instead upregulated at day 14. Indeed, IL-6 is not exclusively involved in the inflammatory response and might also participate in the induction of mechanical hypersensitivity and hyperalgesic priming in different types of arthritis.[49,50,60] The *atf-3* signal was still present at days 7 and 14. Osteoarthritis might be considered as inflammatory disorder, but the resolution of inflammation at the later time points (with histological changes within the bone) and the lack of correlation between *atf-3* and *il-6* transcripts seem to rule out this link. A further assessment of *atf-3* expression at later time points would elucidate whether the pathological changes observed herein fluctuate with time.

Studies in animal OA models have revealed enhanced levels of endocannabinoids in the spinal cord and associated elevations in protein levels of endocannabinoid biosynthetic enzymes.[64] Furthermore, a tonic release of endocannabinoids, which could counteract peripheral sensitization, has been observed.[65,66] Spinal cord levels of AEA and its biosynthetic enzymes were also elevated in a rat OA model.[64] Accordingly, we revealed increased levels of $CB_1$ along with OA development.[62] Considering the location of TRPV1 and $CB_1$ receptors in relation to nociceptive transmission,[30,57,67] both have attracted attention during the development of new treatments for OA pain. Herein, we showed an ipsilateral alteration of FAAH mRNA in the L4–L6 DRG 7 days after the induction of OA. Furthermore, the quantitative real-time PCR data indicated that the expression of TRPV1 mRNA was not altered during the development of OA.

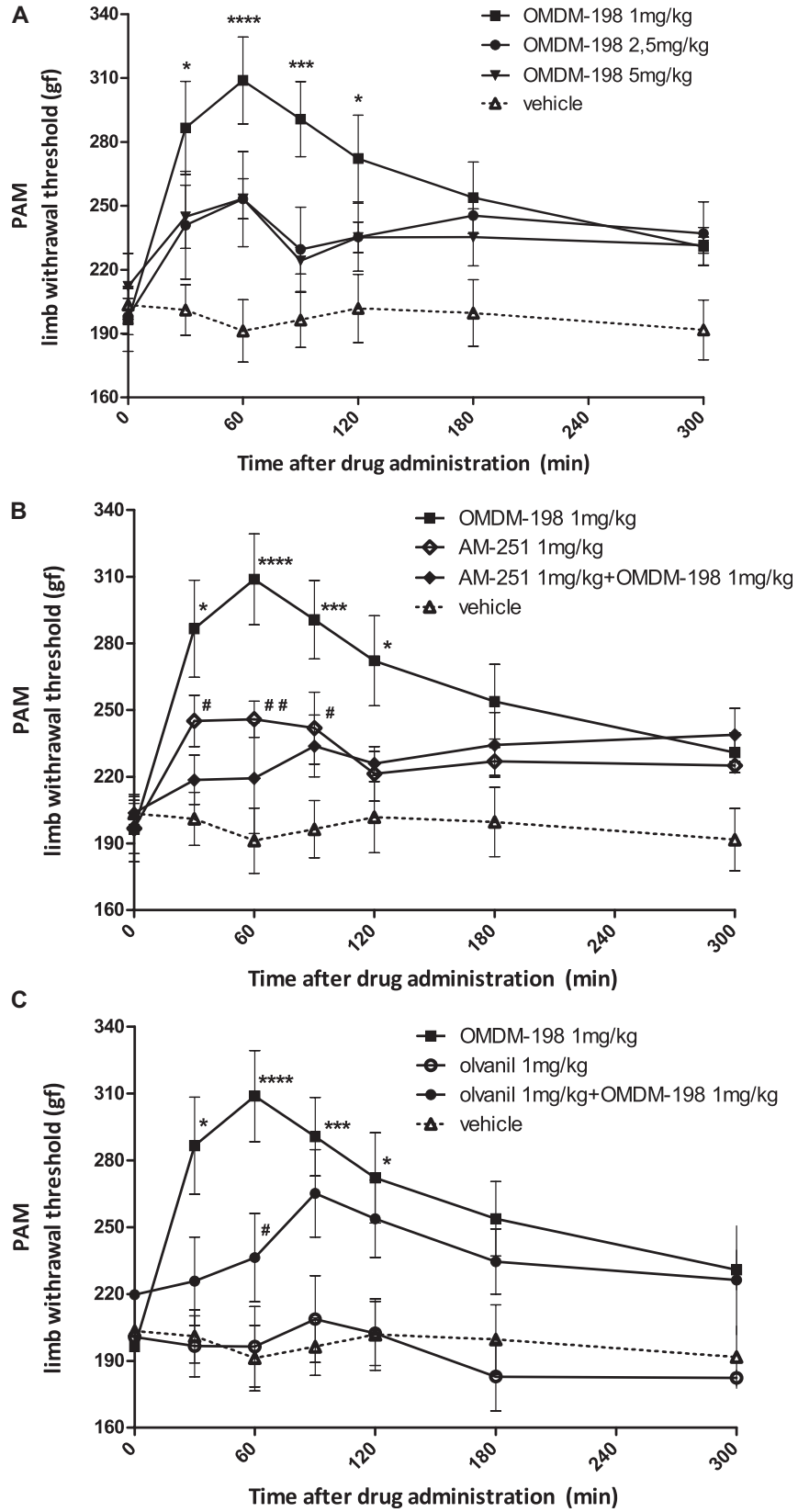


**Figure 8.** Effect of acute systemic treatment with OMDM-198 (1-5 mg/kg, i.p.), alone (A) or in combination (B, C) with AM-251 (1 mg/kg, i.p.) or olvanil (1 mg/kg, i.p.) on hind limb joint hypersensitivity in osteoarthritic rats. Fourteen days after injection with 3 mg of MIA, the rats received OMDM-198 (1-5 mg/kg), and the hind limb withdrawal threshold was assessed over a 300-minute period. A systemic preadministration of the $CB_1$ receptor antagonist AM-251 (1 mg/kg) and of the TRPV1 receptor antagonist olvanil (1 mg/kg) significantly reduced the analgesic effect of OMDM-198. A statistical analysis was performed using a one-way analysis of variance followed by Bonferroni post hoc test. The values with $P < 0.05$ were considered significant. * denotes significant differences vs vehicle, # denotes significant differences vs OMDM-198 (1 mg/kg). The values are the means ± SEM.

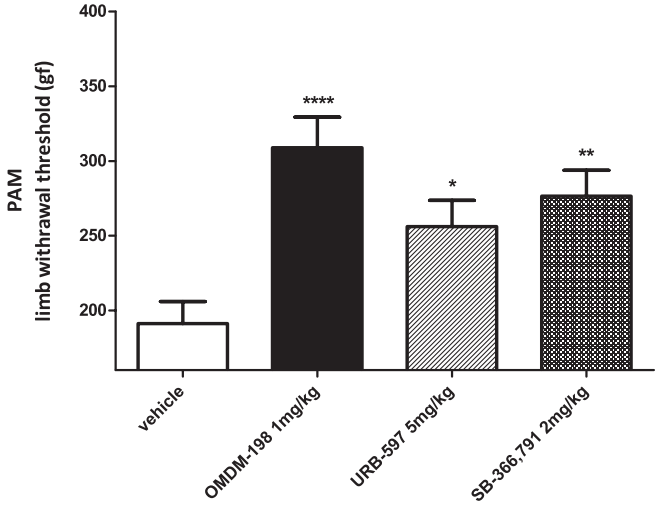


**Figure 9.** Comparison of the analgesic effects of OMDM-198 with those of the FAAH inhibitor, URB-597, and the TRPV1 receptor antagonist, SB-366,791, on hind limb joint hypersensitivity in MIA-treated rats. Fourteen days after injection with 3 mg of MIA, the rats received OMDM-198 (1 mg/kg), URB-587 (5 mg/kg), or SB-366,791 (2 mg/kg), and the hind limb withdrawal threshold was evaluated 60 minutes after administration. A statistical analysis was performed using a one-way analysis of variance followed by Bonferroni post hoc tests. The values with $P < 0.05$ were considered significant. * denotes significant differences vs vehicle. The values are the means ± SEM.

However, an alteration in the DRG at day 2 was observed. Some of the observed changes were bilateral, suggesting that unilateral arthritis can induce bilateral changes.[19] OMDM-198 primary targets, ie, TRPV1 and FAAH, were largely co-expressed at the protein level in the cell bodies of afferent neurons innervating the joint, thus providing the histological basis for the effectiveness of OMDM-198. In fact, we observed a high number of cells displaying TRPV1/$CB_1$ and TRPV1/FAAH immunoreactivity. However, no functional upregulation of the number of cells co-expressing either TRPV1/$CB_1$ or TRPV1/FAAH was observed in the MIA-induced model of OA pain. Changes in protein expression in knee-innervating cells could be obscured by the unchanged expression of proteins in cells that do not contribute to the innervation of the knee, thus explaining this latter finding.

Because of the analgesic and anti-inflammatory properties[40,48] of cannabinoids, their effects have been studied in animal models of arthritis. Nonpsychoactive cannabinoids, such as cannabidiol (CBD) and HU-320, can reduce joint damage and inflammation in murine collagen-induced arthritis,[47,70] suggesting their potential as therapeutic agents for arthritis. The presence of the endocannabinoid system in the synovium suggests that its targeting could be also a therapeutic strategy for the treatment of OA. Accordingly, preventing AEA breakdown in neuronal and non-neuronal cells was shown to produce beneficial effects for the treatment of osteoarthritic pain through both anti-inflammatory and antihyperalgesic actions.[1,39] Regardless of these promising pharmacological advances to treat arthritis and associated hyperalgesia with FAAH inhibitors, PF-04457845 failed to produce an effective analgesia against OA pain in a randomized placebo-controlled phase II clinical trial.[33] A possible explanation is the fact that not all the physiological effects of endocannabinoids are mediated by $CB_1$ and $CB_2$ receptors.[58,68] Endocannabinoids also produce their effects through TRPV1 desensitization, which has been shown to be effected also by phytocannabinoids, including CBD.[6] TRPV1 desensitization also mediates anti-inflammatory effects in a rat model of acute inflammation in which the TRPV1 antagonist capsazepine reversed the effects of CBD, whereas $CB_1$ (SR141716A)- and $CB_2$ (SR144528)-specific antagonists had no effect.[13] Recently, a noxious effect of FAAH inhibitors, ie, AEA-induced cell death, was observed in human cardiomyocytes.[52] Thus, the inhibition of FAAH could result in negative effects by increasing the production of endocannabinoids, leading to liver and myocardial injury.

A new class of dual-acting compounds that simultaneously elevate endogenous FAAH substrates' levels and inactivate TRPV1 receptors is a promising approach for pain relief.[14] The present results support the idea that the systemic administration of a dual FAAH/TRPV1 blocker can reduce joint pain evoked by an injection of MIA. Indeed, throughout the time course of this study, OMDM-198 exhibited a significant reversal of joint hypersensitivity. OMDM-198 was effective only at the lowest tested dose, and this could be because the full inhibition of FAAH, which likely occurs at higher doses, may generate the production of anandamide derivatives with proalgesic actions,[23,58,69] or may produce levels of anandamide that activate TRPV1 too strongly for this effect to be antagonized by the simultaneous effect of the drug on TRPV1 (particularly because OMDM198 is less potent as FAAH inhibitor than as TRPV1 antagonist, and its effect on FAAH might become more important at high doses). The lack of effect of OMDM198 at 5 mg/kg might be due also to the prevalence of activation of anandamide off targets (and not just TRPV1[57]) over TRPV1 antagonism. However, we showed that the analgesic effect of the 1 mg/kg dose of OMDM-198 was due to indirect agonism of $CB_1$ and antagonism of the TRPV1 receptors, as indicated by its counteraction by per se inactive doses of AM-251, a $CB_1$ blocker that may behave as an inverse agonist, and olvanil, a TRPV1 receptor agonist. A $CB_2$ antagonist, AM-630, did not affect the OMDM-198 analgesic profile (Supplementary Fig. 1, available online as Supplemental Digital Content at http://links.lww.com/PAIN/A49). OMDM-198 was recently demonstrated to have both central and peripheral sites of action in formalin and carrageenan tests in mice and to act through TRPV1 antagonism and the elevation of endocannabinoid levels.[31] When OMDM-198 efficacy was compared here to that of URB-597, a selective FAAH inhibitor, and of SB-366,791, a selective TRPV1 antagonist, the optimal doses required to achieve a comparable analgesic effect were much higher for the 2 single-target drugs than for OMDM-198.

In summary, the model of intra-articular MIA injections provides a preclinical tool in which consistent pain readouts are inhibited by OMDM-198, a synthetic compound that inhibits FAAH and antagonizes TRPV1. Our results may lead to an innovative pharmacotherapic strategy for OA.

## Conflict of interest statement

The authors have no conflicts of interest to declare.

This work was supported by the Sonata Bis UMO-2012/07/E/NZ7/01269 grant and statutory funds. N. Malek is a recipient of a scholarship from the KNOW, which is sponsored by the Ministry of Science and Higher Education, Poland.

## Acknowledgements

The authors thank Agnieszka Pajak and Magdalena Kostrzewa for their expert technical assistance. Vincenzo Di Marzo and Katarzyna Starowicz contributed equally to this study.

## Appendix A. Supplemental Digital Content

Supplemental Digital Content associated with this article can be found online at http://links.lww.com/PAIN/A49.

**Article history:**
Received 18 September 2014
Received in revised form 30 January 2015
Accepted 2 February 2015
Available online 20 February 2015

## References

[1] Ahn K, Smith SE, Liimatta MB, Beidler D, Sadagopan N, Dudley DT, Young T, Wren P, Zhang Y, Swaney S, Van Becelaere K, Blankman JL, Nomura DK, Bhattachar SN, Stiff C, Nomanbhoy TK, Weerapana E, Johnson DS, Cravatt BF. Mechanistic and pharmacological characterization of PF-04457845: a highly potent and selective fatty acid amide hydrolase inhibitor that reduces inflammatory and noninflammatory pain. J Pharmacol Exp Ther 2011;338:114–24.

[2] Baker CL, McDougall JJ. The cannabinomimetic arachidonyl-2-chloroethylamide (ACEA) acts on capsaicin-sensitive TRPV1 receptors but not cannabinoid receptors in rat joints. Br J Pharmacol 2004;142:1361–7.

[3] Barton NJ, Strickland IT, Bond SM, Brash HM, Bate ST, Wilson AW, Chessell IP, Reeve AJ, McQueen DS. Pressure application measurement (PAM): a novel behavioural technique for measuring hypersensitivity in a rat model of joint pain. J Neurosci Methods 2007;163:67–75.

[4] Binkowski M, Davis GR, Wrobel Z, Goodship AE. 6th World Congress of Biomechanics (WCB 2010). August 1-6, 2010 Singapore. Lim CT, Goh JCH, editors. Berlin, Heidelberg: Springer Berlin Heidelberg, 2010. p. 856–859.

[5] Binkowski M, Kokot G, Bolechala F, John A. Image-based finite element modeling of the three-point bending test of cortical bone. In: Stock SR, editor. Proc. SPIE 8506, developments in x-ray tomography VIII, 85060D, 2012. p. 85060D.

[6] Bisogno T, Hanus L, De Petrocellis L, Tchilibon S, Ponde DE, Brandi I, Moriello AS, Davis JB, Mechoulam R, Di Marzo V. Molecular targets for cannabidiol and its synthetic analogues: effect on vanilloid VR1 receptors and on the cellular uptake and enzymatic hydrolysis of anandamide. Br J Pharmacol 2001;134:845–52.

[7] Bisogno T, Melck D, De Petrocellis L, MYu Bobrov, Gretskaya NM, Bezuglov VV, Sitachitta N, Gerwick WH, Di Marzo V. Arachidonoyl serotonin and other novel inhibitors of fatty acid amide hydrolase. Biochem Biophys Res Commun 1998;248:515–22. Available at: http://www.ncbi.nlm.nih.gov/pubmed/9703957.

[8] Bjordal JM, Klovning A, Ljunggren AE, Slørdal L. Short-term efficacy of pharmacotherapeutic interventions in osteoarthritic knee pain: A meta-analysis of randomised placebo-controlled trials. Eur J Pain 2007;11:125–38.

[9] Bove SE, Calcaterra SL, Brooker RM, Huber CM, Guzman RE, Juneau PL, Schrier DJ, Kilgore KS. Weight bearing as a measure of disease progression and efficacy of anti-inflammatory compounds in a model of monosodium iodoacetate-induced osteoarthritis. Osteoarthritis Cartilage 2003;11:821–30. Available at: http://www.ncbi.nlm.nih.gov/pubmed/14609535.

[10] Burr DB, Gallant MA. Bone remodelling in osteoarthritis. Nat Rev Rheumatol 2012;8:665–73.

[11] Chang L, Luo L, Palmer JA, Sutton S, Wilson SJ, Barbier AJ, Breitenbucher JG, Chaplan SR, Webb M. Inhibition of fatty acid amide hydrolase produces analgesia by multiple mechanisms. Br J Pharmacol 2006;148:102–13.

[12] Chu KL, Chandran P, Joshi SK, Jarvis MF, Kym PR, McGaraughty S. TRPV1-related modulation of spinal neuronal activity and behavior in a rat model of osteoarthritic pain. Brain Res 2011;1369:158–66.

[13] Costa B, Colleoni M, Conti S, Trovato AE, Bianchi M, Sotgiu ML, Giagnoni G. Repeated treatment with the synthetic cannabinoid WIN 55,212-2 reduces both hyperalgesia and production of pronociceptive mediators in a rat model of neuropathic pain. Br J Pharmacol 2004;141:4–8.

[14] Costa SKP, Teles AM, Kumagai Y, Brain SD, Teixeira SA, Varriano AA, Barreto MAG, de Lima WT, Antunes E, Muscará MN. Involvement of sensory nerves and TRPV1 receptors in the rat airway inflammatory response to two environment pollutants: diesel exhaust particles (DEP) and 1,2-naphthoquinone (1,2-NQ). Arch Toxicol 2010;84:109–17.

[15] Cravatt BF, Demarest K, Patricelli MP, Bracey MH, Giang DK, Martin BR, Lichtman AH. Supersensitivity to anandamide and enhanced endogenous cannabinoid signaling in mice lacking fatty acid amide hydrolase. Proc Natl Acad Sci U S A 2001;98:9371–6.

[16] Cui M, Honore P, Zhong C, Gauvin D, Mikusa J, Hernandez G, Chandran P, Gomtsyan A, Brown B, Bayburt EK, Marsh K, Bianchi B, McDonald H, Niforatos W, Neelands TR, Moreland RB, Decker MW, Lee C-H, Sullivan JP, Faltynek CR. TRPV1 receptors in the CNS play a key role in broad-spectrum analgesia of TRPV1 antagonists. J Neurosci 2006;26:9385–93.

[17] Cyganik Ł, Binkowski M, Kokot G, Rusin T, Popik P, Bolechała F, Nowak R, Wróbel Z, J A. Prediction of Young' s modulus of trabeculae in microscale using macro-scale' s relationships between bone density and mechanical properties. J Mech Behav Biomed Mater 2014;36C:120–34.

[18] DiMarzo V. Inhibitors of endocannabinoid breakdown for pain: not so FA(AH)cile, after all. PAIN 2012;153:1785–6.

[19] Donaldson LF. Unilateral arthritis: contralateral effects. Trends Neurosci 1999;22:495–6. Available at: http://www.ncbi.nlm.nih.gov/pubmed/10530993.

[20] Fernihough J, Gentry C, Malcangio M, Fox A, Rediske J, Pellas T, Kidd B, Bevan S, Winter J. Pain related behaviour in two models of osteoarthritis in the rat knee. PAIN 2004;112:83–93.

[21] Filipek J, Binkowski M, Maciejewska K, Drzazga Z, Wróbel Z. Investigation of microstructure of bone tissue in mandibles of newborn rats after maternal treatment with antiretroviral drugs. Biocybern Biomed Eng 2014.

[22] Fowler CJ, Tiger G, López-Rodríguez ML, Viso A, Ortega-Gutiérrez S, Ramos JA. Inhibition of fatty acid amidohydrolase, the enzyme responsible for the metabolism of the endocannabinoid anandamide, by analogues of arachidonoyl-serotonin. J Enzyme Inhib Med Chem 2003;18:225–31. Available at: http://www.ncbi.nlm.nih.gov/pubmed/14506913.

[23] Gatta L, Piscitelli F, Giordano C, Boccella S, Lichtman A, Maione S, Di Marzo V. Discovery of prostamide F2α and its role in inflammatory pain and dorsal horn nociceptive neuron hyperexcitability. PLoS One 2012;7:e31111.

[24] Gavva NR, Bannon AW, Hovland DN, Lehto SG, Klionsky L, Surapaneni S, Immke DC, Henley C, Arik L, Bak A, Davis J, Ernst N, Hever G, Kuang R, Shi L, Tamir R, Wang J, Wang W, Zajic G, Zhu D, Norman MH, Louis JC, Magal E, Treanor JJS. Repeated administration of vanilloid receptor TRPV1 antagonists attenuates hyperthermia elicited by TRPV1 blockade. J Pharmacol Exp Ther 2007;323:128–37.

[25] Goldring MB, Marcu KB. Cartilage homeostasis in health and rheumatic diseases. Arthritis Res Ther 2009;11:224.

[26] Guingamp C, Gegout-Pottie P, Philippe L, Terlain B, Netter P, Gillet P. Mono-iodoacetate-induced experimental osteoarthritis: a dose-response study of loss of mobility, morphology, and biochemistry. Arthritis Rheum 1997;40:1670–9.

[27] Guzman RE, Evans MG, Bove S, Morenko B, Kilgore K. Mono-iodoacetate-induced histologic changes in subchondral bone and articular cartilage of rat femorotibial joints: an animal model of osteoarthritis. Toxicol Pathol;31:619–24. Available at: http://www.ncbi.nlm.nih.gov/pubmed/14585729.

[28] Halvorson KG, Sevcik MA, Ghilardi JR, Rosol TJ, Mantyh PW. Similarities and differences in tumor growth, skeletal remodeling and pain in an osteolytic and osteoblastic model of bone cancer. Clin J Pain 2006;22:587–600.

[29] Hannan MT, Felson DT, Pincus T. Analysis of the discordance between radiographic changes and knee pain in osteoarthritis of the knee. J Rheumatol 2000;27:1513–7. Available at: http://www.ncbi.nlm.nih.gov/pubmed/10852280.

[30] Hohmann AG. Spinal and peripheral mechanisms of cannabinoid antinociception: behavioral, neurophysiological and neuroanatomical perspectives. Chem Phys Lipids 2002;121:173–90. Available at: http://www.ncbi.nlm.nih.gov/pubmed/12505699.

[31] Honore P, Chandran P, Hernandez G, Gauvin DM, Mikusa JP, Zhong C, Joshi SK, Ghilardi JR, Sevcik MA, Fryer RM, Segreti JA, Banfor PN, Marsh K, Neelands T, Bayburt E, Daanen JF, Gomtsyan A, Lee CH, Kort ME, Reilly RM, Surowy CS, Kym PR, Mantyh PW, Sullivan JP, Jarvis MF, Faltynek CR. Repeated dosing of ABT-102, a potent and selective TRPV1 antagonist, enhances TRPV1-mediated analgesic activity in rodents, but attenuates antagonist-induced hyperthermia. PAIN 2009;142:27–35.

[32] Honore P, Wismer CT, Mikusa J, Zhu CZ, Zhong C, Gauvin DM, Gomtsyan A, El Kouhen R, Lee C, Marsh K, Sullivan JP, Faltynek CR, Jarvis MF. A-425619 [1-isoquinolin-5-yl-3-(4-trifluoromethyl-benzyl)-urea], a novel transient receptor potential type V1 receptor antagonist, relieves pathophysiological pain associated with inflammation and tissue injury in rats. J Pharmacol Exp Ther 2005;314:410–21.

[33] Huggins JP, Smart TS, Langman S, Taylor L, Young T. An efficient randomised, placebo-controlled clinical trial with the irreversible fatty acid amide hydrolase-1 inhibitor PF-04457845, which modulates endocannabinoids but fails to induce effective analgesia in patients with pain due to osteoarthritis of the knee. PAIN 2012;153:1837–46.

[34] Hunter DJ, Zhang YQ, Niu JB, Tu X, Amin S, Clancy M, Guermazi A, Grigorian M, Gale D, Felson DT. The association of meniscal pathologic

changes with cartilage loss in symptomatic knee osteoarthritis. Arthritis Rheum 2006;54:795–801.
[35] Im HJ, Kim JS, Li X, Kotwal N, Sumner DR, van Wijnen AJ, Davis FJ, Yan D, Levine B, Henry JL, Desevré J, Kroin JS. Alteration of sensory neurons and spinal response to an experimental osteoarthritis pain model. Arthritis Rheum 2010;62:2995–3005.
[36] Janusz MJ, Hookfin EB, Heitmeyer SA, Woessner JF, Freemont AJ, Hoyland JA, Brown KK, Hsieh LC, Almstead NG, De B, Natchus MG, Pikul S, Taiwo YO. Moderation of iodoacetate-induced experimental osteoarthritis in rats by matrix metalloproteinase inhibitors. Osteoarthritis Cartilage 2001;9:751–60.
[37] Jayamanne A, Greenwood R, Mitchell VA, Aslan S, Piomelli D, Vaughan CW. Actions of the FAAH inhibitor URB597 in neuropathic and inflammatory chronic pain models. Br J Pharmacol 2006;147:281–8.
[38] Kinsey SG, Long JZ, O'Neal ST, Abdullah RA, Poklis JL, Boger DL, Cravatt BF, Lichtman AH. Blockade of endocannabinoid-degrading enzymes attenuates neuropathic pain. J Pharmacol Exp Ther 2009;330:902–10.
[39] Kinsey SG, Naidu PS, Cravatt BF, Dudley DT, Lichtman AH. Fatty acid amide hydrolase blockade attenuates the development of collagen-induced arthritis and related thermal hyperalgesia in mice. Pharmacol Biochem Behav 2011;99:718–25.
[40] Klein TW. Cannabinoid-based drugs as anti-inflammatory therapeutics. Nat Rev Immunol 2005;5:400–11.
[41] La Porta C, Bura SA, Negrete R, Maldonado R. Involvement of the endocannabinoid system in osteoarthritis pain. Eur J Neurosci 2014;39: 485–500.
[42] Leuchtweis J, Imhof A-K, Montechiaro F, Schaible H-G, Boettger MK. Validation of the digital pressure application measurement (PAM) device for detection of primary mechanical hyperalgesia in rat and mouse antigen-induced knee joint arthritis. Methods Find Exp Clin Pharmacol 2010;32:575–83.
[43] Limaye A. Drishti: a volume exploration and presentation tool. In: Stock SR, editor. Proc. SPIE 8506, developments in x-ray tomography VIII. 2012. p. 85060X.
[44] Lo GH, Hunter DJ, Zhang Y, McLennan CE, Lavalley MP, Kiel DP, McLean RR, Genant HK, Guermazi A, Felson DT. Bone marrow lesions in the knee are associated with increased local bone density. Arthritis Rheum 2005;52:2814–21.
[45] Maione S, Costa B, Piscitelli F, Morera E, De Chiaro M, Comelli F, Boccella S, Guida F, Verde R, Ortar G, Di Marzo V. Piperazinyl carbamate fatty acid amide hydrolase inhibitors and transient receptor potential channel modulators as "dual-target" analgesics. Pharmacol Res 2013; 76:98–105.
[46] Maione S, De Petrocellis L, de Novellis V, Moriello AS, Petrosino S, Palazzo E, Rossi FS, Woodward DF, Di Marzo V. Analgesic actions of N-arachidonoyl-serotonin, a fatty acid amide hydrolase inhibitor with antagonistic activity at vanilloid TRPV1 receptors. Br J Pharmacol 2007;150:766–81.
[47] Malfait AM, Gallily R, Sumariwalla PF, Malik AS, Andreakos E, Mechoulam R, Feldmann M. The nonpsychoactive cannabis constituent cannabidiol is an oral anti-arthritic therapeutic in murine collagen-induced arthritis. Proc Natl Acad Sci U S A 2000;97:9561–6.
[48] Mbvundula EC, Rainsford KD, Bunning RAD. Cannabinoids in pain and inflammation. Inflammopharmacology 2004;12:99–114. doi:10.1163/1568560041352275.
[49] Melemedjian OK, Tillu D V, Moy JK, Asiedu MN, Mandell EK, Ghosh S, Dussor G, Price TJ. Local translation and retrograde axonal transport of CREB regulates IL-6-induced nociceptive plasticity. Mol Pain 2014;10: 45. doi:10.1186/1744-8069-10-45.
[50] Miller RE, Miller RJ, Malfait AM. Osteoarthritis joint pain: the cytokine connection. Cytokine 2014.
[51] Morera E, De Petrocellis L, Morera L, Moriello AS, Ligresti A, Nalli M, Woodward DF, Di Marzo V, Ortar G. Synthesis and biological evaluation of piperazinyl carbamates and ureas as fatty acid amide hydrolase (FAAH) and transient receptor potential (TRP) channel dual ligands. Bioorg Med Chem Lett 2009;19:6806–9.
[52] Mukhopadhyay P, Horváth B, Rajesh M, Matsumoto S, Saito K, Bátkai S, Patel V, Tanchian G, Gao RY, Cravatt BF, Haskó G, Pacher P. Fatty acid amide hydrolase is a key regulator of endocannabinoid-induced myocardial tissue injury. Free Radic Biol Med 2011;50:179–95.
[53] Naidu PS, Kinsey SG, Guo TL, Cravatt BF, Lichtman AH. Regulation of inflammatory pain by inhibition of fatty acid amide hydrolase. J Pharmacol Exp Ther 2010;334:182–90.
[54] Neogi T, Felson D, Niu J, Lynch J, Nevitt M, Guermazi A, Roemer F, Lewis CE, Wallace B, Zhang Y. Cartilage loss occurs in the same subregions as subchondral bone attrition: a within-knee subregion-matched approach from the Multicenter Osteoarthritis Study. Arthritis Rheum 2009;61:1539–44.
[55] Ortar G, Cascio MG, De Petrocellis L, Morera E, Rossi F, Schiano-Moriello A, Nalli M, de Novellis V, Woodward DF, Maione S, Di Marzo V. New N-arachidonoylserotonin analogues with potential "dual" mechanism of action against pain. J Med Chem 2007;50:6554–69.
[56] Patricelli MP, Lashuel HA, Giang DK, Kelly JW, Cravatt BF. Comparative characterization of a wild type and transmembrane domain-deleted fatty acid amide hydrolase: identification of the transmembrane domain as a site for oligomerization. Biochemistry 1998;37:15177–87.
[57] Pertwee RG. Cannabinoid receptors and pain. Prog Neurobiol 2001;63: 569–611. Available at: http://www.ncbi.nlm.nih.gov/pubmed/11164622.
[58] Piscitelli F, Di Marzo V. "Redundancy" of endocannabinoid inactivation: new challenges and opportunities for pain control. ACS Chem Neurosci 2012;3:356–63.
[59] Pomonis JD, Boulet JM, Gottshall SL, Phillips S, Sellers R, Bunton T, Walker K. Development and pharmacological characterization of a rat model of osteoarthritis pain. PAIN 2005;114:339–46.
[60] Price TJ. Targeting eIF4E phosphorylation for the prevention and treatment of chronic pain. 15th World Congress on Pain, Topical Workshop no.27. Buenos Aires, Argentina, 2014.
[61] Puttfarcken PS, Han P, Joshi SK, Neelands TR, Gauvin DM, Baker SJ, Lewis LGR, Bianchi BR, Mikusa JP, Koenig JR, Perner RJ, Kort ME, Honore P, Faltynek CR, Kym PR, Reilly RM. A-995662 [(R)-8-(4-methyl-5-(4-(trifluoromethyl)phenyl)oxazol-2-ylamino)-1,2,3,4-tetrahydronaphthalen-2-ol], a novel, selective TRPV1 receptor antagonist, reduces spinal release of glutamate and CGRP in a rat knee joint pain model. PAIN 2010;150: 319–26.
[62] Richardson D, Pearson RG, Kurian N, Latif ML, Garle MJ, Barrett DA, Kendall DA, Scammell BE, Reeve AJ, Chapman V. Characterisation of the cannabinoid receptor system in synovial tissue and fluid in patients with osteoarthritis and rheumatoid arthritis. Arthritis Res Ther 2008;10:R43.
[63] Robinson I, Sargent B, Hatcher JP. Use of dynamic weight bearing as a novel end-point for the assessment of Freund's Complete Adjuvant induced hypersensitivity in mice. Neurosci Lett 2012;524:107–10.
[64] Sagar DR, Staniaszek LE, Okine BN, Woodhams S, Norris LM, Pearson RG, Garle MJ, Alexander SPH, Bennett AJ, Barrett DA, Kendall DA, Scammell BE, Chapman V. Tonic modulation of spinal hyperexcitability by the endocannabinoid receptor system in a rat model of osteoarthritis pain. Arthritis Rheum 2010;62:3666–76.
[65] Schuelert N, Johnson MP, Oskins JL, Jassal K, Chambers MG, McDougall JJ. Local application of the endocannabinoid hydrolysis inhibitor URB597 reduces nociception in spontaneous and chemically induced models of osteoarthritis. PAIN 2011;152:975–81.
[66] Schuelert N, McDougall JJ. Cannabinoid-mediated antinociception is enhanced in rat osteoarthritic knees. Arthritis Rheum 2008;58:145–53.
[67] Starowicz K, Cristino L, Di Marzo V. TRPV1 receptors in the central nervous system: potential for previously unforeseen therapeutic applications. Curr Pharm Des 2008;14:42–54. Available at: http://www.ncbi.nlm.nih.gov/pubmed/18220817.
[68] Starowicz K, Di Marzo V. Non-psychotropic analgesic drugs from the endocannabinoid system: "magic bullet" or "multiple-target" strategies? Eur J Pharmacol 2013;716:41–53.
[69] Starowicz K, Makuch W, Korostynski M, Malek N, Slezak M, Zychowska M, Petrosino S, De Petrocellis L, Cristino L, Przewlocka B, Di Marzo V. Full inhibition of spinal FAAH leads to TRPV1-mediated analgesic effects in neuropathic rats and possible lipoxygenase-mediated remodeling of anandamide metabolism. PLoS One 2013;8:e60040.
[70] Sumariwalla PF, Gallily R, Tchilibon S, Fride E, Mechoulam R, Feldmann M. A novel synthetic, nonpsychoactive cannabinoid acid (HU-320) with antiinflammatory properties in murine collagen-induced arthritis. Arthritis Rheum 2004;50:985–98.
[71] Tétreault P, Dansereau M-A, Doré-Savard L, Beaudet N, Sarret P. Weight bearing evaluation in inflammatory, neuropathic and cancer chronic pain in freely moving rats. Physiol Behav 2011;104:495–502.
[72] Tonge DP, Pearson MJ, Jones SW. The hallmarks of osteoarthritis and the potential to develop personalised disease-modifying pharmacological therapeutics. Osteoarthritis Cartilage 2014;22:609–21.
[73] Tsujino H, Kondo E, Fukuoka T, Dai Y, Tokunaga A, Miki K, Yonenobu K, Ochi T, Noguchi K. Activating transcription factor 3 (ATF3) induction by axotomy in sensory and motoneurons: A novel neuronal marker of nerve injury. Mol Cell. Neurosci 2000;15:170–82.
[74] Valdes AM, De Wilde G, Doherty SA, Lories RJ, Vaughn FL, Laslett LL, Maciewicz RA, Soni A, Hart DJ, Zhang W, Muir KR, Dennison EM, Wheeler M, Leaverton P, Cooper C, Spector TD, Cicuttini FM, Chapman V, Jones G, Arden NK, Doherty M. The Ile585Val TRPV1 variant is involved in risk of painful knee osteoarthritis. Ann Rheum Dis 2011;70:1556–61.
[75] Zimmermann M. Ethical guidelines for investigations of experimental pain in conscious animals. PAIN 1983;16:109–10. Available at: http://www.ncbi.nlm.nih.gov/pubmed/6877845.